北大巴山地区斑鸠关组砂岩地球化学特征对物源和构造环境的限定

张英利，王宗起，王坤明，王刚，武昱东
中国地质科学院矿产资源研究所自然资源部成矿作用与资源评价重点实验室，北京，100037

内容提要：北大巴山是南秦岭造山带的重要组成部分，保留较完整的地层记录。长期以来，斑鸠关组被认为形成于相对稳定的构造环境。本文通过对斑鸠关组砂岩的沉积序列和地球化学分析，详细分析其物源区和形成构造环境。沉积学特征表明，斑鸠关组砂岩主要为一套深水沉积的细砂岩、粉砂岩和泥岩组合序列，形成于海底扇。砂岩中交错层理恢复的古流向表明，其物源主要来自于北侧。地球化学分析表明，斑鸠关组砂岩 SiO_2 为 61.54%～84.35%，主要为成熟度较低的岩屑砂屑岩。稀土元素标准化配分曲线呈现轻稀土富集、重稀土平坦和 Eu 负异常的特征。砂岩的风化蚀变指数为 51～67，Th/U 比值为 3.36～7.02，表明砂岩物源区经历了较弱的风化作用。Zr/Sc 和 Th/Sc 比值指示斑鸠关组砂岩没有经历沉积再旋回，为近源沉积。砂岩物源区组成判别图表明，斑鸠关组物源主要为长英质岩石。砂岩源区构造环境判别图以及特征指数表明，斑鸠关组源区形成于大陆岛弧和被动大陆边缘环境。综合区域资料，表明斑鸠关组形成于大陆岛弧相关环境，非大陆裂谷。

关键词：北大巴山；斑鸠关组；地球化学；物源分析；构造环境

从新元古代到至今，南秦岭造山带经历了俯冲增生造山（Yan Zhen et al.，2006，2010，2011，2012；Wang Zongqi et al.，2009；Lin Zhenwen et al.，2013；Wang Kunming et al.，2015；Wang Gang et al.，2017）和板内碰撞造山过程（Sun Weidong et al.，2003；Zhang Chengli et al.，2008；Lei Min et al.，2011）。然而，关于其早古生代造山过程仍然存在争议。北大巴山位于南秦岭造山带南部，以城口断裂为界与南大巴山隔开。北大巴山主要由古生代灰岩、碎屑岩和火山碎屑岩等组成（Zhang Yingli et al.，2016；Wang Gang et al.，2017）。长期以来，依据火山岩的地球化学特征，将北大巴山早古生代的构造环境解释为不同的观点，一种观点认为早古生代时期岩石圈拉张，处于伸展构造环境（大陆裂谷或被动大陆边缘）（Teng Renlin et al.，1990；Huang Yuehua et al.，1992；Xia Zuchun et al.，1992；Gao Changlin，1993；Zhang Chengli et al.，2003；Chen Gaochao et al.，2011；Zou Xianwu et al.，2011；Dong Yunpeng et al.，2013；Wan Jun et al.，2016；Yang Cheng et al.，2017；Zhang Guishan et al.，2017）；近年来随着新资料的发现，则认为早古生代时期发育洋岛/海山的沉积序列（Wang Zongqi et al.，2009；Yan Zhen et al.，2011），为弧后环境（Wang Zongqi et al.，2009；Wang Kunming et al.，2015，2016；Xu Guang et al.，2018）或洋岛环境（Chen Youzhang et al.，2010；Yan Zhen et al.，2011）或大洋板内环境（Xiang Zhongjin et al.，2010）。

砂岩碎屑组成受多种因素控制，包括源岩成分、构造环境、风化作用、搬运以及成岩作用等（McLennan et al.，1993）。然而，构造环境和源区母岩成分是沉积岩的最主要控制因素（Bhatia，1983；Roser et al.，1988；McLennan et al.，1993；Roser，2000；Garzanti et al.，2007）。因此，根据碎屑岩的地球化学特征，前人已经建立物源和构造环境的相互联系（Bhatia，1983；Roser et al.，1986，

注：本文为中国地质调查项目（编号 12120114009401，DD20190099）和国家自然科学基金项目（编号 41302080，41602061）资助成果。
收稿日期：2019-04-02；改回日期：2019-07-27；网络发表日期：2019-11-04；责任编委：任东；责任编辑：黄敏。
作者简介：张英利，男，1979年生。副研究员，主要从事沉积学与盆地构造研究。Email：yinglizh@126.com。

引用本文：张英利，王宗起，王坤明，王刚，武昱东. 2020. 北大巴山地区斑鸠关组砂岩地球化学特征对物源和构造环境的限定. 地质学报，94(4)：1192～1207，doi：10.19762/j.cnki.dizhixuebao.2020014.
Zhang Yingli，Wang Zongqi，Wang Kunming，Wang Gang，Wu Yudong. 2020. Sandstone geochemical constraints on the provenance and tectonic setting of the Banjiuguan Formation in the North Daba Mountain. Acta Geologica Sinica，94(4)：1192～1207.

1988;McLennan et al.,1991;Jorge et al.,2013)。斑鸠关组碎屑岩为研究北大巴山构造演化提供了很好的物质基础。

本文研究针对北大巴山地区斑鸠关组地层,通过野外地质特征的调查,并运用地球化学等方法,阐述斑鸠关组物源区以及岩石性质,同时限定北大巴山地区古生代的构造环境,进而为南秦岭造山带的古生代构造演化提供依据。

1　地质背景

秦岭造山带经历了增生造山和陆内造山过程(Wang Zongqi et al.,2009),形成了今日的构造格局,分别以商丹缝合带和勉略缝合带为界,分为北秦岭、中秦岭和南秦岭三部分(图 1b),以城口断裂为界,在南秦岭和扬子构造单元划分出北大巴山和南大巴山。北大巴山作为南秦岭最主要的构造单元之

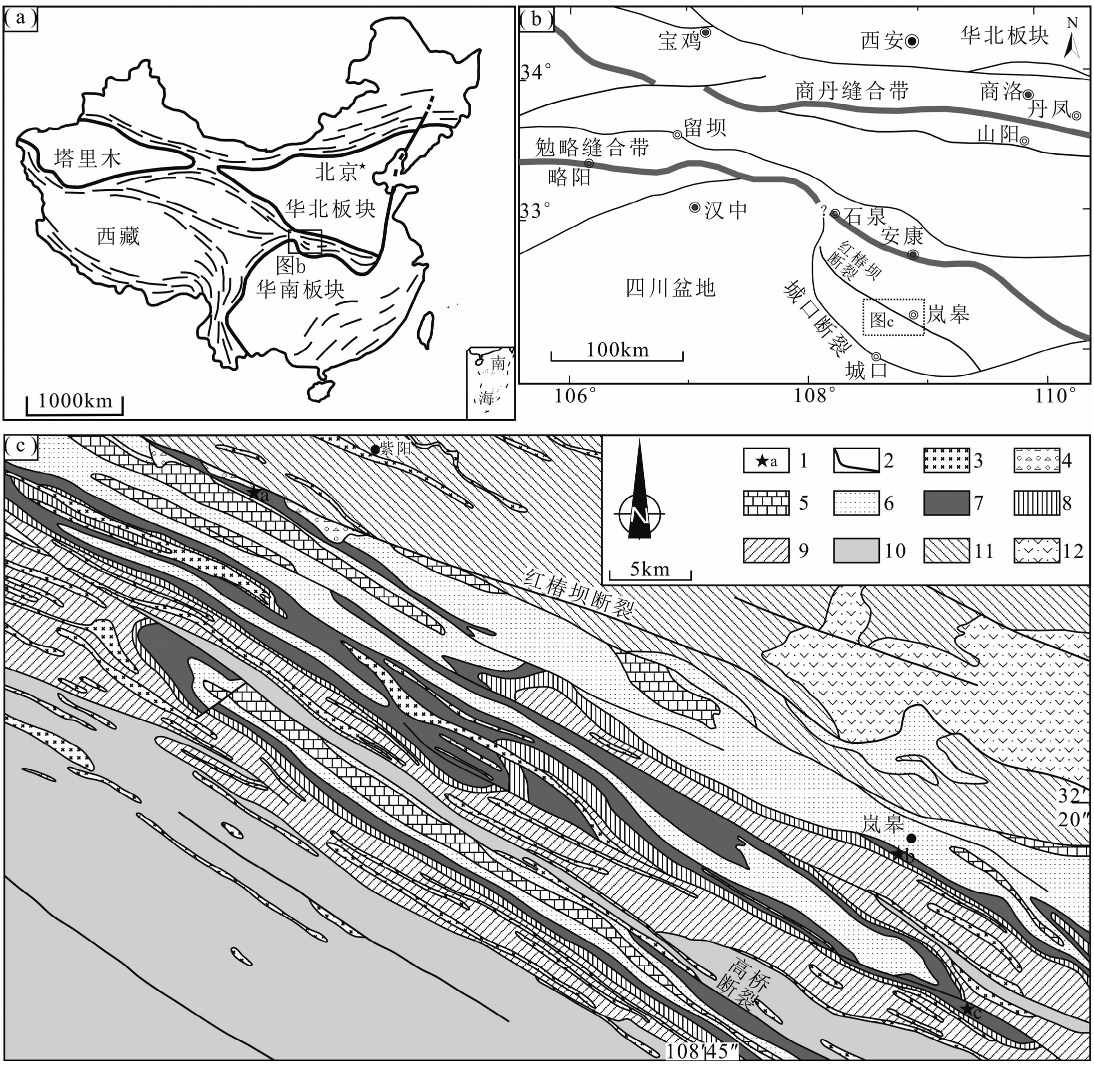

图 1　北大巴山地区地质简图

(a)—研究区构造位置,据 Mattauer et al.,1985;(b)—构造单元划分,据 Wang Zongqi et al.,2009;

(c)—研究区地质图,据 1/5 万洞河幅、佐龙幅和岚皋幅修改

Fig. 1　Simplified geological map in the North Daba Mountains

(a)—tectonic location, modified from Mattauer et al., 1985; (b)—division of tectonic units, modified from Wang Zongqi et al., 2009; (c)—simplified geological map, modified from the 1/50 000 regional geological report of Donghe, Zuolong and Langao Mapsheet

1—剖面位置;2—断层;3—辉绿岩;4—侏罗系;5—五峡河组;6—陡山沟组;7—斑鸠关组;8—权河口组;9—高桥组;10—寒武系;11—洞河群;12—耀岭河群

1—section location; 2—fault; 3—diabase; 4—Jurassic; 5—Wuxiahe Formation; 6—Doushangou Formation; 7—Banjiuguan Formation; 8—Quanhekou Formation; 9—Gaoqiao Formation; 10—Cambrian; 11—Donghe Group; 12—Yaolinghe Group

一,以红椿坝断裂为界,研究区划分为两个不同的构造单元(图 1b,c),其地层组成也不同(表 1)。断裂以北为洞河群,由粘土质板岩、灰质板岩和部分碳质板岩等组成,夹火山碎屑岩、粗面岩等,鉴定出晚古生代化石(Wang Zongqi et al.,2009)。耀岭河群下部为含砾中酸性凝灰岩夹流纹英安岩、绿泥片岩,上部斜长绿泥片岩、绢云绿泥片岩,顶部为钙质千枚岩、中性火山角砾岩、变玄武岩和斜长片岩等,火山岩的锆石年龄指示其形成于新元古代(Zhu Xiyan et al.,2014)。

红椿坝断裂以南古生界自下而上主要由寒武系、奥陶系高桥组、奥陶纪—志留纪权河口组和斑鸠关组及泥盆系滔河口组/陡山沟组和五峡河组构成(表 1)。其中,寒武系由深水沉积的灰岩组成,高桥组主要为灰、灰黑色板岩、钙质板岩,夹薄层或条带状泥质灰岩,含笔石;权河口组主要由两部分组成:下部为以条带状碳质板岩为主,含笔石、三叶虫、腕足化石,上部为灰黑色、绿灰色粉砂质板岩夹粉(细)砂岩、长石石英砂岩。斑鸠关组以黑色碳质板岩、碳质硅质板岩为主,夹砂岩及粗面火山岩;陡山沟组(与滔河口组同期异相)以灰色砂岩、粉砂岩为主,夹少量板岩和玄武质火山岩,碎屑锆石测年和 Ar-Ar 同位素分析结果表明,滔河口组形成于泥盆纪(Zhang Yingli et al., 2016; Wang Gang et al., 2017)。陡山沟组之上的五峡河组为灰色粉砂质板岩、黑色碳质板岩夹粉砂岩、碳质粉砂岩。研究区内分布大量铁镁质岩和闪长岩,侵入古生代地层,锆石的 U-Pb 年龄为 399～454Ma(Zhang Chengli et al.,2007;Wang Cunzhi et al.,2009;Zou Xianwu et al., 2011; Wang Kunming et al., 2014; Wang Kunming et al.,2015;Xiang Zhongjin et al.,2016;Zhang Guishan et al.,2017)。

表 1 北大巴山地区地层划分与对比

Table 1 Stratigraphic division and correlation in the North Daba Mountains

红椿坝断裂以南		红椿坝断裂以北	
地层	岩性	地层	岩性
下—中侏罗统	底部为砾岩,下部为砂岩,上部为炭质页岩夹砂岩。	缺失	
五峡河组	灰色粉砂质板岩、黑色碳质板岩夹粉砂岩、碳质粉砂岩。	洞河群(?)	底部以炭质板岩为主,夹炭质灰岩;下部为硅质岩,夹炭质板岩、硅质灰岩;中部以炭质板岩为主;上部以灰色千枚岩为主,夹炭质千枚岩及薄层泥质灰岩。局部夹火山碎屑岩、粗面岩。
滔河口组/陡山沟组	灰色砂岩、粉砂岩为主,夹少量板岩和玄武质火山岩		
斑鸠关组	黑色碳质板岩、碳质硅质板岩为主,夹砂岩及粗面火山岩		
权河口组	下部为以条带状碳质板岩为主,上部为灰黑色、绿灰色粉砂质板岩夹粉(细)砂岩、长石石英砂岩		
高桥组	灰、灰黑色板岩、钙质板岩,夹薄层或条带状泥质灰岩		
寒武系	底部为炭质板岩、硅质岩,灰色厚层泥灰岩、角砾状灰岩		
新元古界	未出露	耀岭河群	下部为含砾中酸性凝灰岩夹流纹英安岩、绿泥片岩,上部斜长绿泥片岩、绢云绿泥片岩,顶部为钙质千枚岩、中性火山角砾岩、变玄武岩和斜长片岩。

斑鸠关组最早称为龙马溪统斑鸠关段、堰沟段,以黑色碳质页岩、灰绿色、灰黑色钙质页岩及粉砂岩为主夹火山岩系(Ma Runhua et al.,1998)。Fu Lipu(1983)将斑鸠关组上部改称为下斑鸠关组,斑鸠关组下部地层因时代属晚奥陶世称为芭蕉口组。Ge Meiyu et al. (1984) 认为斑鸠关组仅包括 *Akidograptus ascensus*—*Spirograptus minor* 笔石带的地层,在紫阳瓦房店以南为灰、灰黑色碳质页岩、泥岩钰硅质泥质粉砂岩互层,中上部夹中薄层砂岩。Fu Lipu(1986)将下斑鸠关组该称为麻柳树湾组。根据区域地层对比和命名优先原则,现在将斑鸠关组定义为以黑色薄—中层砂岩、黑色碳质板岩、碳质硅质板岩为主,夹砂岩及粗面岩(Ma Runhua et al.,1998;Lin Baoyu et al.,1998),且含丰富的笔石化石(Fu Lipu et al.,2004,2006)。与下伏权河口组和上覆陡山沟组均为整合接触。主要分布在紫阳县和岚皋县一带,呈 NW-SE 向条带状分布。

2 沉积特征

斑鸠关组正层型剖面位于紫阳县斑鸠关(现斑桃镇)(Ma Runhua et al,1998),由于植被覆盖等原因,现在难以连续观测斑鸠关组岩性特征。因此,本次研究根据斑鸠关组砂岩的出露分布,自西向东选取渔家崖、头桥和构坪 3 个剖面进行研究(图 1c)。渔家崖剖面位于 32°30′24″,108°27′23″,头桥剖面位于 32°18′23″,108°52′35″,构坪剖面位于 32°13′17″,108°55′11″。

渔家崖剖面(图 2a)厚度 15.2m,下部主要为深

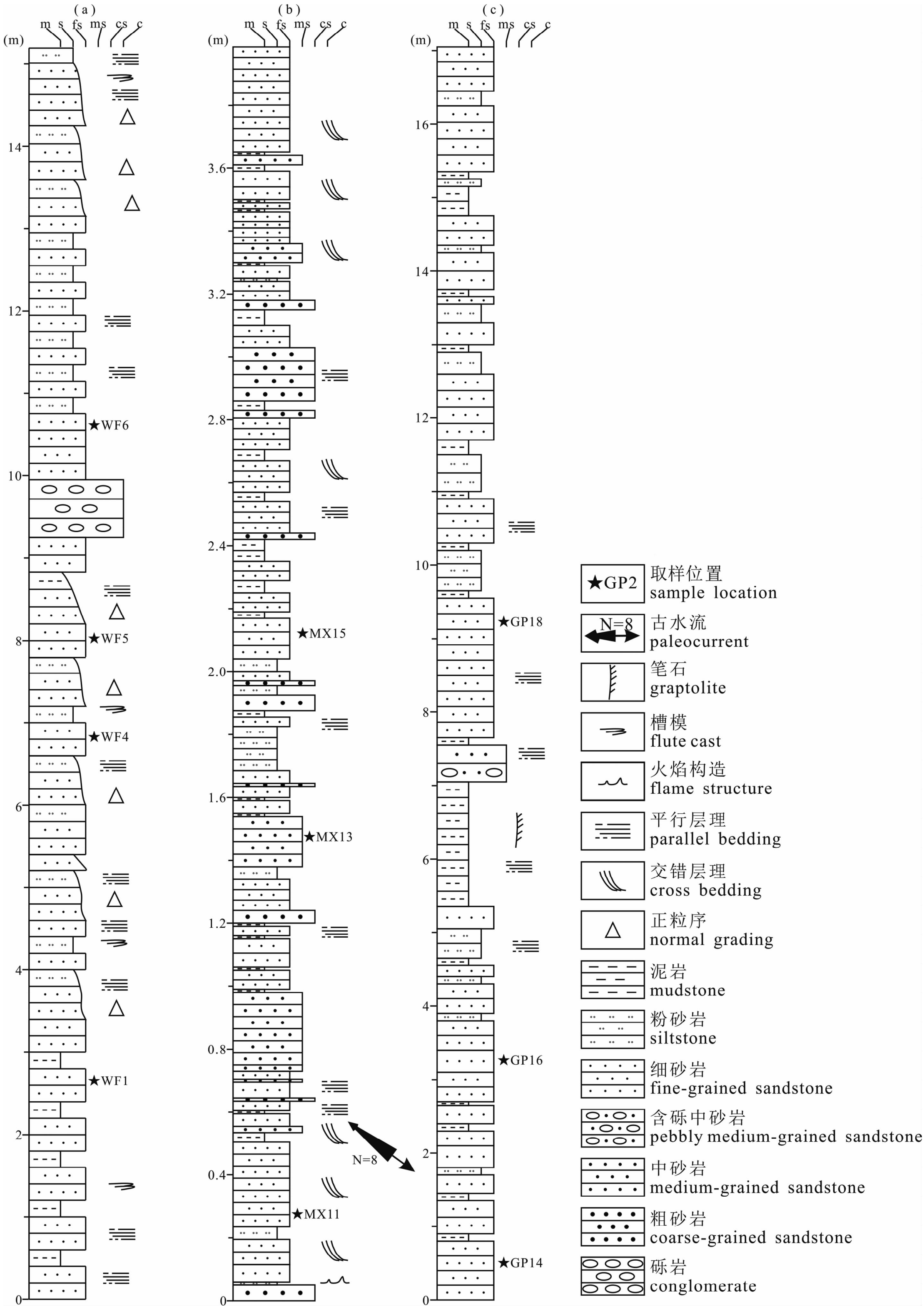

图 2　北大巴山地区斑鸠关组砂岩沉积序列图(剖面位置见图 1)

Fig. 2　Sedimentary successions of Banjiuguan Formation in the North Dabashan area (Location of section are indicated in Fig. 1)

(a)—渔家崖剖面;(b)—头桥剖面;(c)—构坪剖面

m—泥岩;s—粉砂岩;fs—细砂岩;ms—中砂岩;cs—粗砂岩;c—砾岩

(a)—Yujiaya Section; (b)— Touqiao Section; (c)— Gouping Section

m—mudstone; s—siltstone; fs—fine-grained sandstone; ms—medium-grained sandstone; cs—coarse-grained sandstone; c—conglomerate

灰色中一厚层细砂岩夹灰黑色薄层泥岩、粉砂岩(图3ab)。砂岩呈透镜状,发育平行层理和粒序层理(图3c),底部见槽模构造(图3d)。中部为灰黑色厚层细砾岩(0.70m),基质支撑。砾石砾径2～30cm,成分主要为灰黑色泥岩、少量为深灰色砂岩。可见黄铁矿。上部为深灰色中层细砂岩与薄层灰黑色粉砂岩互层,细砂岩单层厚层约15～20cm,粉砂岩5～6cm,自底向顶粉砂岩逐渐变厚。细砂岩发育平行层理、粒序层理和槽模构造。粉砂岩发育正粒序。因此,剖面砂岩发育正粒序层理、槽模构造和平行层理指示浊流沉积,粉砂岩发育水平层理,以背景悬浮沉积为主。砂岩与粉砂岩组成的岩石组合,指示主要为浊流沉积,构成鲍玛序列的不同Tb、Td段。中部基质支撑砾岩杂乱、无粒序层理,砾石成分为泥岩和砂岩,则指示碎屑流沉积作用(Nardin et al.,1979;Lowe,1982;Talling et al.,2004,2012)。

头桥剖面(图2b)厚度3.99m,以深灰色细砂岩为主,局部夹深灰色粗砂岩和灰黑色泥岩、粉砂岩。细砂岩发育火焰构造(图3e)和平行层理、交错层理(图3f),局部发育逆粒序和同沉积正断层(图3f),底部见冲刷面(图3f)。粗砂岩底部可见砾石,部分粉砂岩/泥岩中可见少量砾石。因此,头桥剖面砂岩发育逆粒序、火焰构造和平行层理指示浊流沉积,粉砂岩发育水平层理,以背景悬浮沉积为主。砂岩、粉砂岩组成的岩石组合,构成鲍玛序列的不同Tc、Td段。中砂岩局部含砾,且几乎不发育沉积构造,其可能为高密度浊流或(液化)碎屑流沉积成因(Talling et al.,2012;Shanmugam,2015)。

构坪剖面(图2c)厚度17.05m。下部主要为灰绿色厚层细砂岩夹灰绿色薄层泥岩、粉砂岩,细砂岩发育平行层理。中部为灰绿色薄层泥岩,发育水平层理,见大量笔石化石。上部主要为灰绿色中层细砂岩、灰绿色薄层粉砂岩和泥岩互层(图3g),局部为含砾中砂岩。细砂岩发育平行层理。黄铁矿较多,沿层面分布。见大量笔石化石(图3h)。因此,粉砂岩发育水平层理,以背景悬浮沉积为主。依据相组合的叠置关系,细砂岩和粉砂岩、泥岩构成鲍玛序列的Tb、Td段。

因此,斑鸠关组碎屑岩主要为浊流和碎屑流成因,岩石组合主要为浊流的不完整的鲍玛序列、无层理砂岩和基质支撑砾岩。渔家崖剖面砂岩/泥岩厚度比是3.29,头桥剖面砂岩/泥岩厚度比值为3.61,而构坪剖面砂岩/泥岩厚度比值相对较小,为1.58。与此同时,渔家崖剖面和头桥剖面斑鸠关组垂向上出现浊流一碎屑流一浊流的重力流转化,这种现象在其他海底扇的沉积物中也有大量报道(McCaffrey et al.,2001;Haughton et al.,2003;Lowe et al.,2003;Talling et al.,2004;Georgiopoulou et al.,2009)。因此,根据其岩石组合、岩石厚度比值等,其沉积环境为海底扇的扇中。这与前人关于南秦岭斑鸠关组泥页岩为深水陆棚的结论基本一致(Xiong Guoqing et al.,2017)。

3 样品描述和分析方法

3.1 样品描述

鉴于岩石风化程度、出露情况等,在渔家崖剖面、头桥剖面和构坪剖面分别采集斑鸠关组砂岩样品3块、3块和4块(图2)。

3.2 分析方法

砂岩样品碎样加工在河北省区域地质矿产调查研究所实验室完成,无污染粉碎至200目。岩石全岩由国家地质实验中心完成,主量元素在飞利浦PW2404 X射线荧光光谱仪上完成,微量元素和稀土元素在Finningan MAT的HR-ICP-MS(Element Ⅰ)上进行,分析精度优于5%。

4 岩石地球化学特征

4.1 主量元素

不同剖面的斑鸠关组砂岩主量元素含量相似,差别不明显。SiO_2含量在主量元素中最高,介于61.54%～84.35%。与其他元素表现出不同程度的相关性:Al_2O_3(相关系数$\gamma=-0.86$),Fe_2O_3($\gamma=-0.86$),MnO($\gamma=-0.29$),MgO($\gamma=-0.82$),CaO($\gamma=0.09$),Na_2O($\gamma=-0.34$)和K_2O($\gamma=-0.62$)。SiO_2与CaO为正相关,表明少量碳酸盐为次生。Al_2O_3含量介于6.06%～13.31%,Al_2O_3与K_2O呈正相关($\gamma=0.76$),表明高Al_2O_3含量主要与粘土矿物有关。CaO含量普遍低于1%,较高含量的CaO可能与局部少量方解石胶结有关。Fe_2O_3和MgO之间呈正相关($\gamma=0.85$),表明元素主要受铁镁质矿物影响。而且,Fe_2O_3和TiO_2之间相关系数为0.89,表明元素富集受Fe-Ti氧化物控制。

埋藏成岩作用导致长石和岩屑的破坏、不稳定矿物的溶解以及次生加大等,原始的物理和化学条件再平衡改变了砂岩成分。对于较粗碎屑岩,成岩作用导致不稳定组分溶解、迁移。长石对于环境敏感,易于发生溶解。同时,成岩作用也会导致碳酸盐岩屑的溶解和白云岩化、火山岩岩屑绿泥石化等

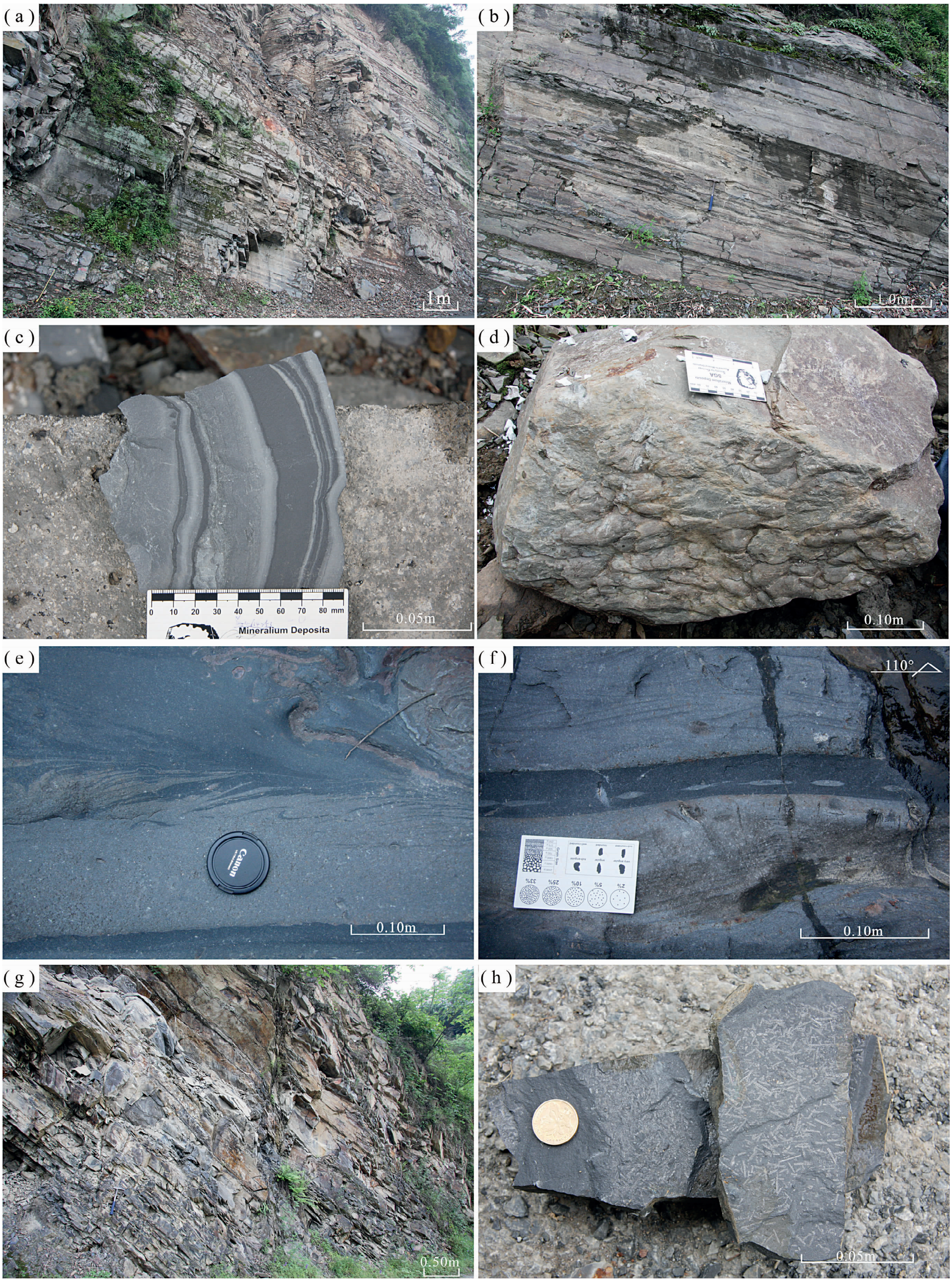

图 3　北大巴山斑鸠关组砂岩野外典型照片

Fig. 3　Typical photographs of Banjiuguan sandstone in the North Dabashan Mountain

(a)—渔家崖剖面剖面全貌;(b)—渔家崖剖面细砂岩与粉砂岩;(c)—渔家崖剖面粒序层理;(d)—渔家崖剖面槽模,(e)—头桥剖面火焰构造;(f)—头桥剖面平行层理、粒序层理和冲刷面;(g)—构坪剖面细砂岩与粉砂岩;(h)—构坪剖面的笔石化石

(a)—Yujiaya section; (b)—fine-grained sandstone and siltstone developed in the Yujiaya secton; (c)—grading bedding of sandstone developed in the Yujiaya section; (d)—flute structure of sandstone developed in the Yujiaya section; (e)—flame structure of sandstone in the Touqiao section; (f)—parallel bedding, grading bedding and erosional surface in the Touqiao section; (g)—fine-grained sandstone and siltstone developed in the Gouping secton; (h)—graptolite in sandstone of Gouping section

(Johnsson,1993)。根据砂岩中主量元素与矿物的相互关系:K 元素与钾长石和云母等含钾矿物有关,Si 元素反映硅酸盐(尤其是石英)的含量,Fe、Mg、Mn 和 Ti 等主要表明基性岩屑和副矿物的特征。Al 与 K 正相关,表明砂岩成岩作用过程中形成粘土矿物。另外,较高含量的 CaO 可能与成岩作用过程中方解石胶结有关。

4.2 微量元素和稀土元素

砂岩中 Rb 含量为 $55\pm14\times10^{-6}$,表明富集一定程度的细粒泥质颗粒。Sr 含量介于 $39\sim339\times10^{-6}$,表明源区风化程度较低。Ba 含量较高,普遍 $>200\times10^{-6}$。Zr 含量 $163\times10^{-6}\sim697\times10^{-6}$,Hf 含量 $6\sim17\times10^{-6}$,二者呈正相关($\gamma=1$),表明出现重矿物锆石。砂岩具有不同的 Th 和 U 含量,Th/U 比值为 3.36~7.02。

在风化作用、低级变质和热液蚀变过程中,稀土元素不活泼。砂岩的 ∑REE 介于 $182\times10^{-6}\sim391\times10^{-6}$ 之间,平均为 243×10^{-6}。δEu 值介于 0.48~0.66,平均 0.61。La/Yb 在 12.15~19.78 之间,平均为 14.35。∑LREE/∑HREE 介于 7.26~12.36,平均为 8.43。∑REE 和 Zr 呈正相关($\gamma=0.77$),表明稀土元素主要富集于碎屑矿物(可能为锆石等)。∑REE 和 TiO_2 亦呈正相关($\gamma=0.87$),反映沉积物中富集含钛矿物(如金红石)。尽管不同样品的稀土元素含量变化较大,澳大利亚后太古宙平均页岩(PAAS)标准化,斑鸠关组样品表现出平坦配分模式(La_N/Yb_N 平均 7.29,6.17~10.05),具有弱的 Ce 异常(δCe 平均为 1.00)和明显的 Eu 负异常(平均值 0.94)(图 4a,表 2)。球粒陨石标准化配分模式以轻稀土富集、重稀土平坦和铕负异常为特征(图 4b)。

5 讨论

5.1 砂岩类型

砂岩 SiO_2 含量为 61.54%~84.35%(平均为 74.29%)表明样品中石英含量差异显著。Al_2O_3 含量为 6.06~13.31%(平均为 9.87%),$Fe_2O_3{}^T$ 含量为 2.37~9.87%(平均 4.43%),K_2O 含量为 0.84~4.13%(平均为 1.91%)。$Fe_2O_3{}^T/K_2O$ 比值为 2.48 ± 0.94,矿物的稳定性差。根据 Herron(1988)陆源碎屑岩岩石类型划分方案,斑鸠关组砂岩分析样品主要为岩屑砂屑岩和硬砂岩,个别为铁页岩(图 5a)。根据 Pettijohn et al. (1972)划分方案,砂岩样品绝大多数为岩屑砂屑岩,构坪剖面个别砂岩样品为亚长石砂岩(图 5b)。砂岩分类图解表明,样品的成熟度较低,砂岩沉积物未经过长距离搬运,近源堆积。

5.2 风化作用和分选

砂岩成分虽然主要受母岩区岩石性质决定,但

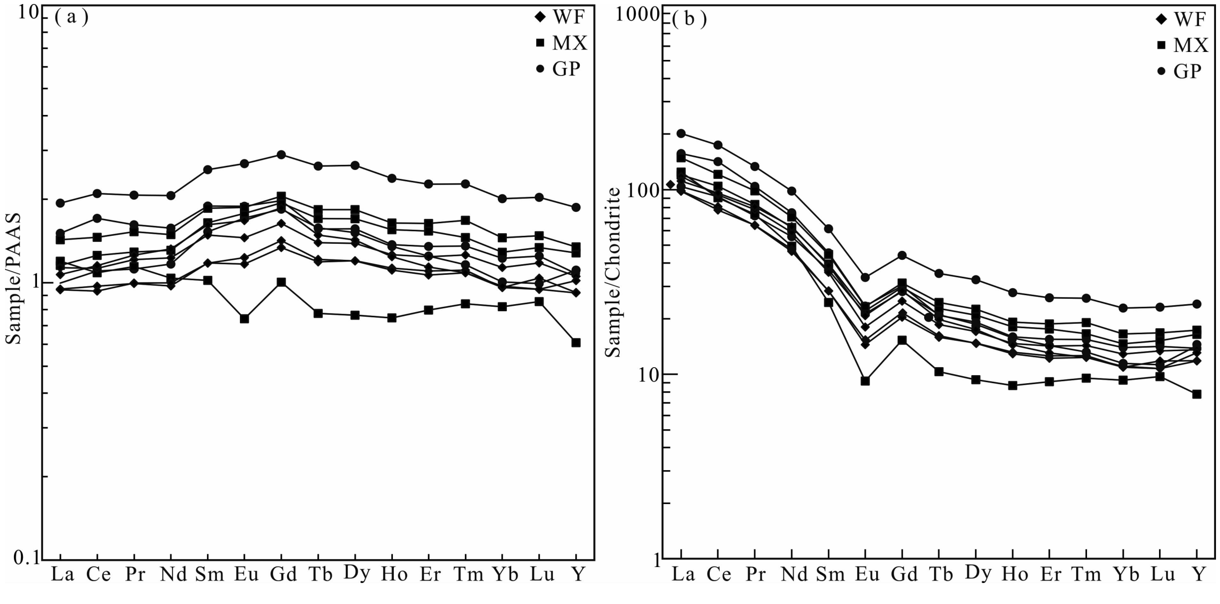

图 4 北大巴山斑鸠关组砂岩 PAAS 曲线(a)和稀土元素配分曲线(b)

Fig. 4 Post-Archaean Average Shale (PAAS) (a) and chondrite-normalized (b) REE diagrams for the Banjiuguan Formation sandstones in the North Dabashan Mountain

(a)和(b)标准化值分别采用澳大利亚后太古宙平均页岩(McLennan,1989)和球粒陨石(Taylor and McLennan,1985)

Normalized values are from McLennan (1989) and Taylor and McLennan (1985)

表 2　北大巴山斑鸠关组砂岩主量元素(%)、微量元素和稀土元素($\times10^{-6}$)含量表

Table 2　Major (%), trace element ($\times10^{-6}$) composition for the Banjiuguan sandstones in the North Daba Mountain

样品	SiO_2	Al_2O_3	Fe_2O_3	MgO	CaO	Na_2O	K_2O	MnO	TiO_2	P_2O_5	LOI	Σ	Sc	V	Cr	Co	Ni	Cu
GP14	84.35	6.06	2.87	0.95	0.50	1.39	0.84	0.04	0.61	0.29	2.00	99.90	5.76	46.20	77.9	6.22	20.9	10.3
GP16	61.54	13.31	9.87	2.60	0.43	2.14	2.13	0.08	2.57	0.34	3.92	98.93	21.2	287	216	17.8	47.7	32.1
GP18	77.24	9.33	4.00	1.33	0.37	1.60	1.66	0.03	0.78	0.19	2.63	99.16	7.91	57.5	64.6	5.13	14.5	12.1
MX11	74.82	10.01	4.54	1.40	0.52	1.92	1.63	0.06	0.64	0.32	3.26	99.12	8.97	61.1	56.3	6.75	20.5	10.5
MX13	68.54	12.18	5.65	2.79	0.19	1.67	4.13	0.03	0.63	0.09	2.55	98.45	11.70	105	69.9	13.4	52.4	21.6
MX15	71.94	11.57	4.56	1.38	0.35	3.21	2.68	0.03	0.87	0.19	1.85	98.63	10.60	76.5	72.7	14	37.1	18.7
WF1	78.4	8.79	2.76	1.03	1.73	2.22	1.28	0.06	0.61	0.17	2.52	99.57	6.92	45.5	43	7.2	21.2	11.9
WF4	73.96	7.18	2.37	0.86	5.40	1.70	1.11	0.09	0.67	0.21	5.52	99.07	6.02	38.6	43.3	5.18	17.2	13.5
WF5	76.11	10.40	4.23	1.40	0.36	1.78	1.90	0.04	0.61	0.18	2.07	99.08	7.97	56.8	47.2	12	30.1	18.1
WF6	76.04	9.89	3.45	1.24	1.47	1.95	1.72	0.06	0.61	0.17	2.48	99.08	8.15	54.9	48.2	9.98	26.6	19.5

Ga	Rb	Sr	Y	Nb	Cs	Ba	La	Ce	Pr	Nd	Sm	Eu	Gd	Tb	Dy	Ho	Er	Tm	Yb	Lu	Ta	Pb	Th	U	Zr	Hf
8.02	27.7	42.8	30	17.6	1.71	201	38.1	87.7	9.89	39.6	8.48	1.85	8.59	1.22	7.1	1.34	3.56	0.47	2.84	0.43	1.05	8.73	7.19	1.14	180	5.69
22.2	71.8	72.6	50.5	123	3.72	842	74	167	18.3	70	14.2	2.91	13.5	2.04	12.4	2.36	6.47	0.92	5.67	0.88	6.21	14.1	12.1	2.96	697	17.3
13.4	55.5	43.2	29.1	40.7	3.29	382	57.6	136	14.3	53.4	10.5	2.04	9.21	1.21	7.32	1.36	3.85	0.55	3.46	0.54	3.01	11	13.4	2.27	397	11
13	55.4	55.7	34.6	15.7	3.57	425	44.1	100	11.4	44.4	9.13	1.92	9.05	1.32	7.96	1.54	4.38	0.59	3.63	0.58	1.08	8.32	11.8	1.68	245	7.8
17.4	71	39.2	16.4	28.1	2.28	5299	45.7	86.5	10.1	35.2	5.66	0.8	4.68	0.6	3.57	0.74	2.27	0.34	2.31	0.37	2.07	19.8	11.9	3.54	209	6.54
15	60.4	62.6	36.4	43.4	2.72	1991	54.6	116	13.5	50.6	10.3	2.02	9.57	1.42	8.59	1.63	4.67	0.68	4.1	0.64	3.08	18.9	13.5	2.21	371	10
10.4	44.1	130	24.9	10.8	2.41	368	36.2	77.3	8.77	33	6.54	1.26	6.25	0.92	5.62	1.12	3.14	0.45	2.71	0.45	0.89	14	11.4	2.18	289	8.22
8.9	37.8	339	28.5	11.6	2.13	425	43.3	89.7	10.7	41.7	8.25	1.57	7.63	1.08	6.5	1.25	3.54	0.51	3.2	0.51	0.9	12.3	14.2	2.59	530	13.2
13.2	65.3	53.1	27.5	13.5	3.77	678	40.9	91.8	11.1	44.9	8.99	1.81	8.69	1.15	6.67	1.23	3.25	0.44	2.71	0.41	1	10.7	10.3	2.18	163	5.94
12.3	58.9	130	24.8	11.4	3.64	628	36	74.3	8.8	33.9	6.53	1.33	6.61	0.94	5.61	1.1	3.04	0.44	2.74	0.41	0.89	11.2	10.3	2.15	234	7.46

ΣREE	ΣLREE/ΣHREE	La/Yb	(La/Yb)N	Eu/Eu*	Ce/Ce*	K_2O/Na_2O	$\log SiO_2/Al_2O_3$	$\log Na_2O/K_2O$	$\log Fe_2O_3/K_2O$	CIA	PIA	Nb/Y	Zr/TiO_2	Ce*	Cr/Th	Th/Sc
211.17	7.26	13.42	6.82	1.02	1.04	0.60	1.14	0.22	0.53	59.62	61.71	0.59	0.03	1.09	10.83	1.25
390.65	7.83	13.05	6.63	0.99	1.05	1.00	0.66	0.00	0.67	66.83	71.89	2.44	0.03	1.10	17.85	0.57
301.34	9.96	16.65	8.46	0.98	1.09	1.04	0.92	-0.02	0.38	64.65	69.51	1.40	0.05	1.16	4.82	1.69
240.00	7.26	12.15	6.17	0.99	1.03	0.85	0.87	0.07	0.45	63.04	66.77	0.45	0.04	1.08	4.77	1.32
198.84	12.36	19.78	10.05	0.73	0.93	2.47	0.75	-0.39	0.14	61.69	71.37	1.71	0.03	0.99	5.87	1.02
278.32	7.89	13.32	6.77	0.96	0.99	0.83	0.79	0.08	0.23	56.75	59.43	1.19	0.04	1.04	5.39	1.27
183.73	7.89	13.36	6.79	0.93	1.00	0.58	0.95	0.24	0.33	51.79	52.14	0.43	0.05	1.06	3.77	1.65
219.44	8.06	13.53	6.88	0.93	0.96	0.65	1.01	0.19	0.33	51.38	51.67	0.41	0.08	1.01	3.05	2.36
224.05	8.13	15.09	7.67	0.96	0.99	1.07	0.86	-0.03	0.35	64.84	69.96	0.49	0.03	1.04	4.58	1.29
181.75	7.70	13.14	6.68	0.95	0.96	0.88	0.89	0.05	0.30	56.09	57.72	0.46	0.04	1.01	4.68	1.26

注:Fe_2O_3为全铁的含量,化学蚀变指数 CIA= $Al_2O_3/(Al_2O_3+K_2O+Na_2O+CaO^*)\times100$,其中 CaO^* 为校正后的含量(CaO 摩尔数≤Na_2O 摩尔数时,采用 CaO 的值;CaO 摩尔数>Na_2O 摩尔数时,采用 Na_2O 的值 Bock et al.,1998;)稀土元素标准值据 Taylor et al.(1985)。ICV=$(Fe_2O_3+K_2O+Na_2O+CaO+MgO+MnO+TiO_2)/Al_2O_3$(Armstrong-Altrin et al.,2015)。

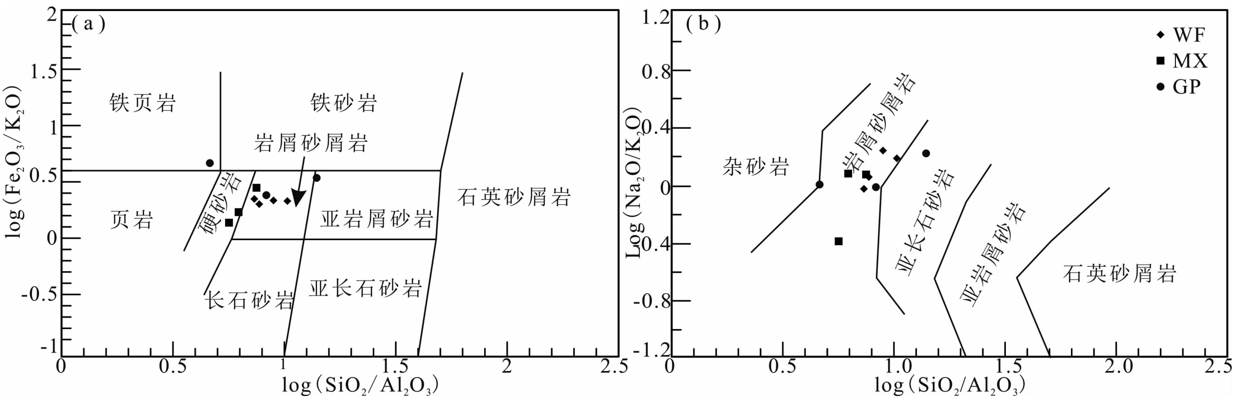

图 5 北大巴山斑鸠关组砂岩分类判别图

Fig. 5 Chemical classification of samples from Banjiuguan sandstones in the North Dabashan Mountain

(a)—log (SiO_2/Al_2O_3) vs. log (Fe_2O_3/K_2O)(据 Herron,1988);(b)—log (SiO_2/Al_2O_3) vs. log (Na_2O/K_2O)(据 Pettijohn et al.,1972)

(a)—log (SiO_2/Al_2O_3) vs. log (Fe_2O_3/K_2O) diagram of Herron(1988);

(b)—log (SiO_2/Al_2O_3) vs. log (Na_2O/K_2O) diagram of Pettijohn et al. (1972)

是风化作用、搬运作用以及成岩作用等过程对其成分影响很大(Johnson,1993)。因此,砂岩的化学成分也能够提供母岩区风化作用的信息。强烈风化作用通常与温暖潮湿气候有关,而干旱气候只是相对较弱化学风化。根据 Nesbit et al.(1984)提出的化学蚀变指数 CIA(Chemical Index of Alteration),CIA 值介于 51～67(表 2),基本与后太古宙页岩的平均 CIA 值相当(图 6a),表明源区的风化作用尚未进行到碱金属和碱土金属从粘土矿物中淋失阶段(Taylor and McLennan,1985)。而且,风化过程中,不稳定元素即 Al 族(Al、Ga),Ti 族(Ti、Zr、Hf)和 REE(包括 Sc、Y)及其他高价离子(Th、Nb)均不受影响。而 Fedo et al.(1995)提出是钾长石蚀变指数 PIA(Plagioclase of Index)的数值为 52～72,表明中等风化程度。将砂岩样品数据投影到 Al_2O_3-(Na_2O+CaO)-K_2O 图解(图 6a),主要位于平均泥岩附近,数据点落在斜长石与伊利石矿物成分的连线附近,表明源区的化学风化主要是斜长石向粘土矿物(伊利石等)的转换过程。表明样品处于中等风化阶段。且风化趋势源于花岗闪长岩,表明沉积物主要来自于长英质源岩。Al_2O_3/Na_2O 比值也是确定风化强度的参数之一(Ali et al.,2014)。斑鸠关组砂岩 Al_2O_3/Na_2O 比值较小(3.60～7.29),表明中等风化程度。

成熟度主要受物理风化和化学风化的改造影响,成分成熟度标志接近终极产物的化学特征。而碎屑岩的成分成熟度可以用参数 ICV(Index of Compositional Variability, Armstrong-Altrin et al.,2015)表示。包含典型岩石形成矿物(长石、角闪石和辉石)的样品 ICV 通常大于 0.84,而包含蚀变矿物(如高岭石、伊利石和白云母等)的样品 ICV 小于 0.84(Cox et al.,1995),因此 ICV 值的降低表明碎屑岩成熟度增加和风化程度的增强。斑鸠关组砂岩 ICV 值>0.99,指示不成熟。而且,砂岩样品多数多富集 CaO(表 2)。在 CIA-ICV 图解(图 6b),样品全部在后太古宙页岩 ICV 趋势线之上,表明其不成熟。这与 A-CN-K 图解的结论一致。

由于 U 的丢失,Th/U 比值随着风化程度的增加而增加,Th/U>4 与风化程度有关(McLennan et al.,1995)。表 2 显示,除样品 MX13 之外,Th/U 比值(4.09～7.02),明显高于上地壳的 Th/U 平均值 3.8(图 7a),表明源区处于中等风化程度。同时,砂岩高 Th/U 比值也可能与源区岩石为长英质岩石有关。

Zr/Sc 和 Th/Sc 比值可以反映沉积物的成分变化、分选情况以及重矿物含量等(McLennan et al.,1993),其比值的正相关关系反映了物源区的成分变化趋势。斑鸠关组砂岩的 Zr 含量为 163×10^{-6}～697×10^{-6}(平均 332×10^{-6}),分布在上地壳周围(平均 190×10^{-6},McLennan,2001),而 Zr/Sc 比值较高的主要原因是 Sc 的浓度远低于上地壳的平均值 14×10^{-6}(McLennan,2001)。Zr/Sc 和 Th/Sc 比值表明绝大多数样品的碎屑组成没有经历再旋回,为近缘沉积(图 7b)。SiO_2/Al_2O_3 比值用于分析沉积物的结构成熟度,比值>10 表示较高的再旋回和高成熟度(Wang Wei et al.,2013)。除 2 个样品之外(分别是 13.92 和 10.30),斑鸠关组砂岩 SiO_2/Al_2O_3 比值多数较低(4.62～8.92),表明较低的成

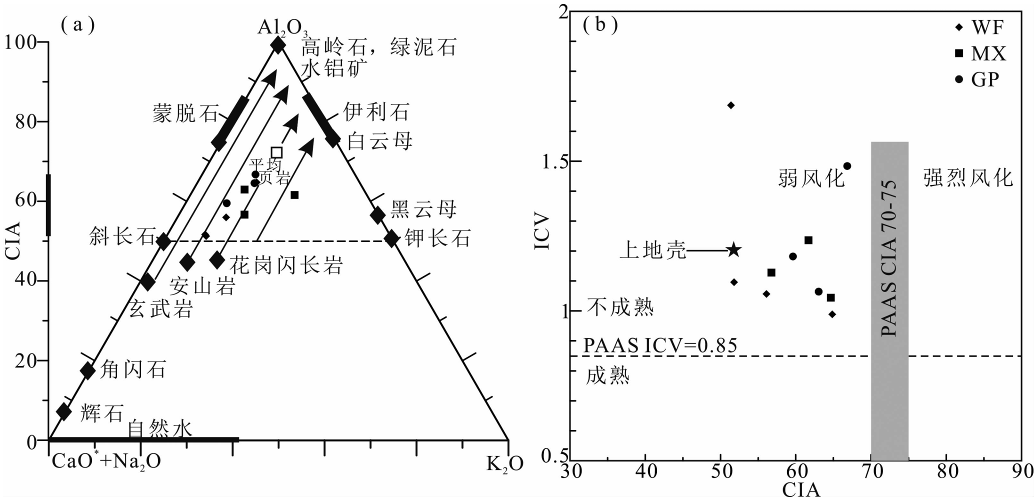

图 6　北大巴山斑鸠关组砂岩 Al_2O_3-(Na_2O+CaO)-K_2O 图解

(a，据 Nesbitt and Young，1984）和 CIA-ICV 图解（b，据 Long Xiaoping et al.，2012)，PAAS—后太古宙平均页岩

Fig. 6　(a) A-CN-K plots showing the weathering trend (after Nesbitt and Young，1984) (b) CIA versus ICV plot show the intensity of weathering and maturity of the siliciclastic sediments of the Banjiuguan Formation in the North Dabashan Mountain (after Long Xiaoping et al.，2012)。PAAS— Post-Archaean Average Shale.

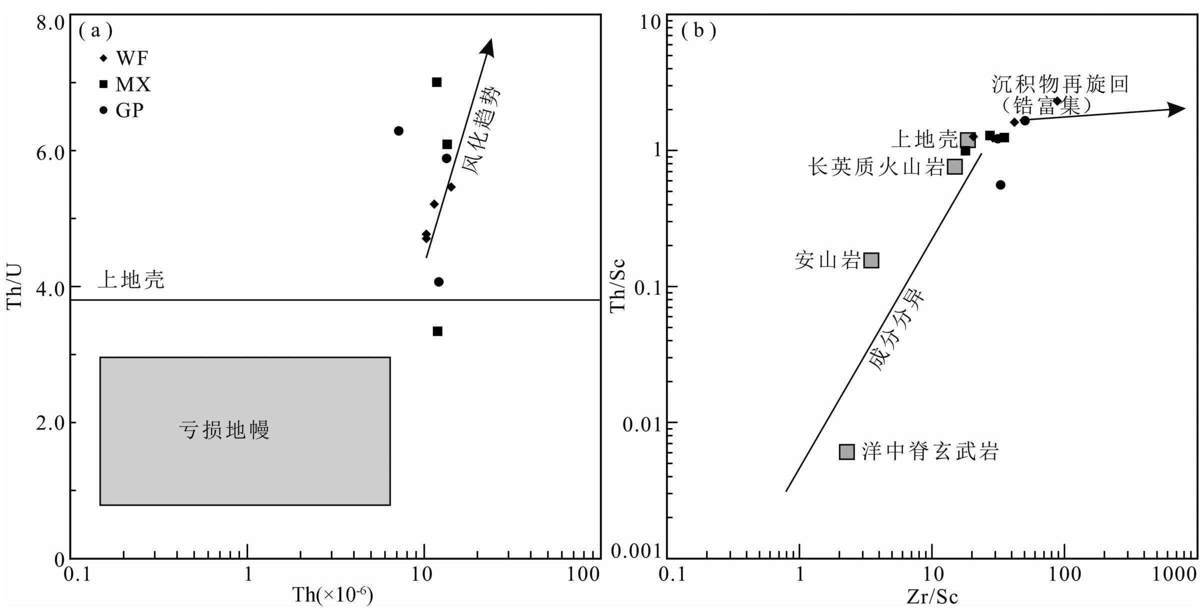

图 7　北大巴山斑鸠关组砂岩 Th/U-Th 图解(a)(据 McLennan et al.，1993)和 Zr/Sc-Th/Sc 图解(b)(据 McLennan et al.，2003)

Fig. 7　Plots of Th/U ration vs. Th abundances (a) (McLennan et al.，1993) and Zr/Sc ratio vs. Th/Sc ratio (b) (McLennan et al.，2003) for the Banjiuguan Formation sandstones in the North Dabashan Mountain

分成熟度。

5.3　源区岩石类型

稀土元素的配分模式反映了沉积物母岩区性质(Taylor et al.，1985；McLennan et al.，1995)。斑鸠关组砂岩具有轻稀土富集、重稀土平坦和铕负异常的稀土元素配分曲线(图 4)，表明沉积母岩主要为长英质。

Hf-La/Th 图解显示，斑鸠关组砂岩具有较为一致的 La/Th 比值(3.05～6.12)和 Hf 含量(5.94～17.3)，表明其物源主要来自于酸性弧环境的岩石，且有较老沉积物成分加入(图 8a)。La/Sc-Co/Th 图解(Gu et al.，2002)，砂岩呈现低且稳定的 Co/Th 比值(0.86)，La/Sc 比值变化较小，指示主要以长英质为主(图 8b)。Zr/TiO_2-Nb/Y 图解表明，砂岩源岩主要为粗面安山岩类和流纹英安岩类(图 8c)。同时，斑鸠关组砂岩的 Th/Sc(0.57～2.36)和

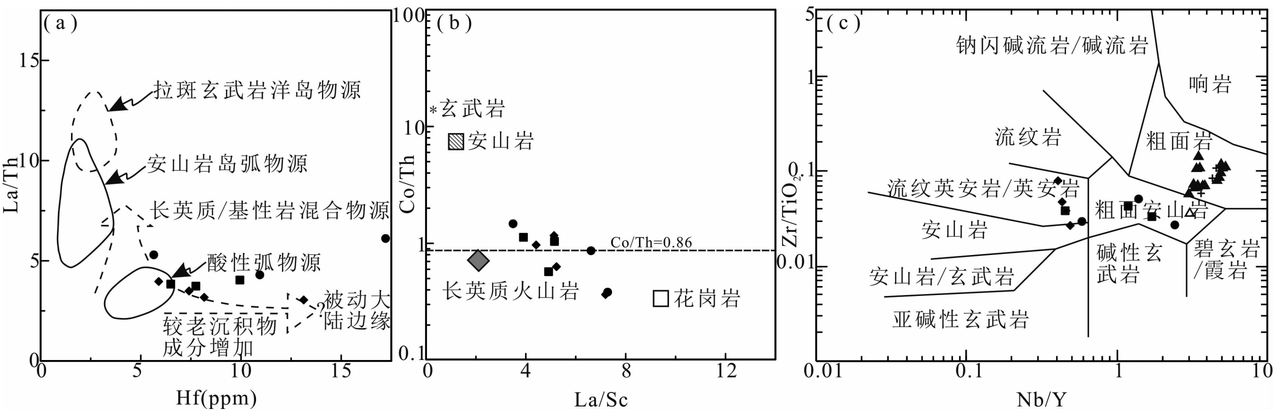

图 8 北大巴山斑鸠关组砂岩沉积物源区判别图

Fig. 8 Discrimination diagrams illustrating sedimentary provenance of the Banjiuguan Formation sandstones in the North Dabashan Mountain

(a)—La/Th-Hf 图解(据 Floyd and Leveridge,1987);(b)—La/Sc-Co/Th 图解(据 Gu et al.,2002);(c)—Nb/Y-Zr/TiO_2图解(据 Winchester and Floyd,1977),△—黄月华等(1992);▲—王刚(2014);+—Zhang Chengli et al.(2003)

(a)—La/Th vs. Hf diagram (Floyd and Leveridge,1987); (b)—La/Sc vs. Co/Th diagram (Gu et al.,2002); (c) —Nb/Y-Zr/TiO_2 diagram (Winchester and Floyd,1977). △—Huang Yuehua et al. (1992); ▲—Wang Gang (2014); +—Zhang Chengli et al. (2003)

La/Sc(3.49～7.28)变化较大,表明物源区为长英质组分。

5.4 潜在物源区

根据地球化学判别图解(图 4,6,7 和 8),斑鸠关组砂岩的源区母岩主要为长英质岩石,主要为粗面安山岩类和流纹英安岩类(图 8c)。根据研究区地层格架和岩浆岩分布情况,其可能的源岩为斑鸠关组砂岩同期的粗面岩或区域上分布闪长岩。区域上闪长岩年龄为 438.4±3.1Ma(Wang Kunming et al.,2015),晚于斑鸠关组砂岩形成时间,不可能为斑鸠关组砂岩的物源。因此,可能的源岩为斑鸠关组砂岩同期的粗面岩。根据斑鸠关组砂岩和火山岩地球化学特征,火山岩多位于粗面岩,砂岩则多为英安岩和粗面安山岩(图 8c)。这可能与火山岩 Nb 含量比砂岩普遍偏高有关。

5.5 构造环境

斑鸠关组砂岩主量元素含量和各种特征化学参数变化范围较宽,$Fe_2O_3{}^T$ + MgO 变化 3.23%～12.47%,平均 6.14%;TiO_2 变化于 0.61%～2.57%,平均 0.92%。将数据投影到 Bhatia(1983)的 $Fe_2O_3{}^T$+MgO-TiO_2 图解,数据点较分散。根据 SiO_2 和 K_2O/Na_2O(Roser and Korsch,1986)图解,大部分样品落入活动大陆边缘(图 9)。然而,GP 2 个样品和 MX 1 个样品落入被动边缘,表明轻矿物(如石英)在源区较富集。

沉积物中微量元素呈现惰性特征,在沉积过程中表现出较弱的变化,因而,其中的一些元素能够较好的反映盆地的构造环境(Taylor et al.,1985;Bhatia,1985;McLennan,2001)。在微量元素建立的 La-Th-Sc、Th-Sc-Zr/10、Th-Co-Zr/10 三角图解(图 10),样品多数落入大陆岛弧区域或附近,少数落入被动大陆边缘区。

根据 Bhatia(1985)总结的不同构造环境砂岩的稀有元素特征值(表 3),将斑鸠关组与之进行对比,其构造背景与大陆岛弧较为接近。

前人依据斑鸠关组和上覆滔河口组岩浆岩的地球化学数据,指示北大巴山早古生代形成于大陆裂谷(被动大陆边缘)(Teng Renlin et al.,1990;Huang Yuehua et al.,1992;Xia Zuchun et al.,1992;Gao Changlin,1993;Zhang Chengli et al.,2003;Zou Xianwu et al.,2011;Dong et al.,2013;Wan Jun et al.,2016;Yang Cheng et al.,2017;Zhang Guishan et al.,2017),然而滔河口组的碎屑锆石则表明其形成于晚古生代(Zhang Yingli et al.,2016)。早古生代辉绿岩等最新的研究成果表明,其形成于俯冲相关的构造环境(Wang Zongqi et al.,2009;Xiang Zhongjin et al.,2010;Wang Kunming et al.,2015,2016;Xu Guang et al.,2018)。

野外调查发现,构坪剖面细砂岩下伏为斑鸠关组粗面岩。头桥剖面下伏和上覆岩石均可见粗面岩。渔家崖剖面上覆和下伏岩石出露较差,未见明显的粗面岩。因此,我们分析的细砂岩样品为火山熔岩间的夹层。也就是说,剖面中碎屑岩为火山喷

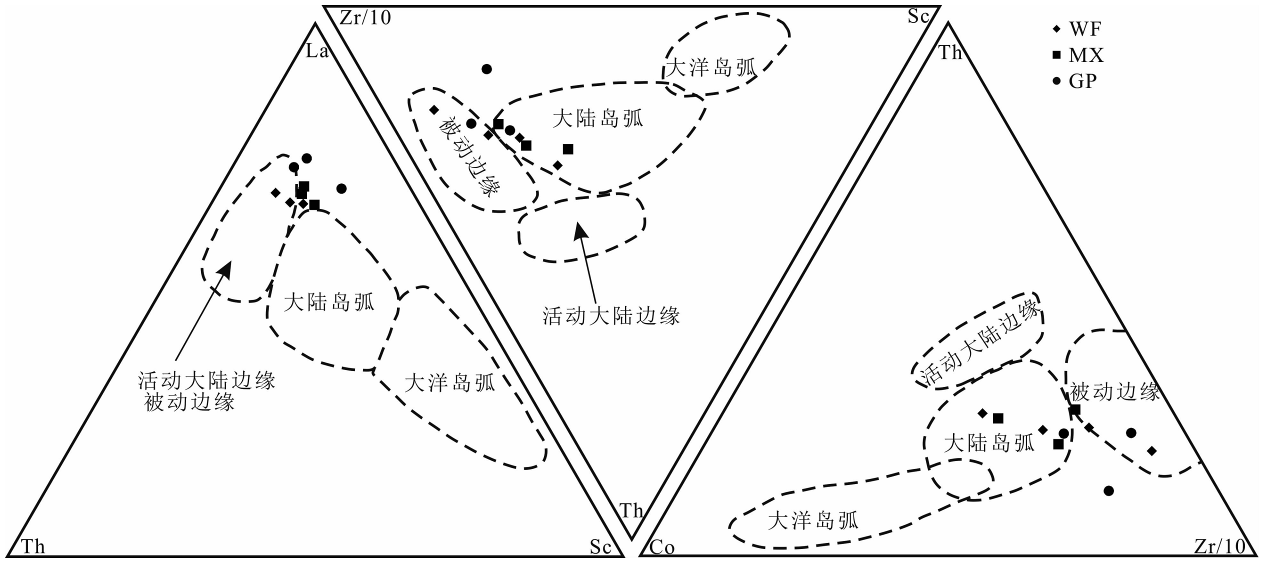

图 9　北大巴山斑鸠关组砂岩 SiO_2 和 K_2O/Na_2O 判别图解(底图据 Roser and Korsch,1986)

Fig. 9　SiO_2 vs. log (K_2O/Na_2O) discrimination diagram introduced by Roser and Korsch (1986) applied to the sandstones from the Banjiuguan Formation in the North Dabashan Mountain

表 3　不同构造背景砂岩的 REE 特征(Bhatia,1985)及与斑鸠关组砂岩对比

Table 3　Discriminating REE characteristics of graywackes for tectonic setting discrimination of sedimentary basins and Banjiuguan Formation sandstones

构造环境	物源类型	REE 参数						
		La	Ce	∑REE	La/Yb	La_N/Yb_N	∑LREE/∑HREE	Eu/Eu*
大洋岛弧	未切割岩浆弧	8±1.7	19±3.7	58±10	4.2±1.3	2.8±0.9	3.8±0.9	1.04±0.11
大陆岛弧	切割岩浆弧	27±4.5	59±8.2	146±20	11.0±3.6	7.5±2.5	7.7±1.7	0.79±0.13
安第斯型陆缘	隆升基底	37	78	186	12.5	8.5	9.1	0.60
被动陆缘	克拉通内部构造高地	39	85	210	15.9	10.8	8.5	0.56
斑鸠关组	切割岩浆弧	47±11.9	103±29.1	243±65	14.4±2.3	9.7±1.5	8.4±1.6	0.61±0.05

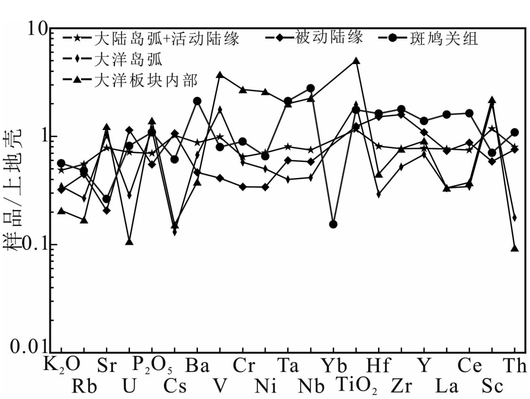

图 10　北大巴山斑鸠关组砂岩 La-Th-Sc、Th-Sc-Zr/10 和 Th-Co-Zr/10 构造背景判别图(Bhatia and Crook,1986)

Fig. 10　Plots of the Banjiuguan Formation sandstones in the North Dabashan Mountain for tectonic discrimination (after Bhatia and Crook, 1986)

发间歇期的产物。其源区构造环境能够指示斑鸠关组粗面岩的形成构造环境。

斑鸠关组物源表示其主要来自于长英质岩石,且 Nb/Y-Zr/TiO_2 判别图解进一步指示,其主要来自粗面安山岩+流纹英安岩/英安岩。这与区域火山岩的地球化学特征基本一致(图 8c),源岩即为斑鸠关组岩浆岩。细砂岩的构造环境判别图解指示源区为大陆岛弧构造环境,这表明斑鸠关组粗面岩形成于大陆岛弧相关的构造环境。与此同时,粗面岩的火山-沉积序列、矿物学特征和岩石地化特征等资料(Wang Gang,2014),证明粗面质火山岩形成于俯冲相关的构造环境。因此,我们有理由认为,斑鸠关组形成于大陆岛弧相关的构造环境。至于进一步准确的限定,需要结合俯冲极性等资料来确定。

斑鸠关组砂岩的物源区判别图解显示,物源区构造背景主要为大陆岛弧,少量为被动大陆边缘。上述分析表明,大陆岛弧的物质来源主要为斑鸠关组的粗面质火山岩。而被动大陆边缘的沉积物可能来自更老的沉积物。在北大巴山地区较老的地层主要是耀岭河群,形成于大陆岛弧环境(Zhu Xiyanet al.,2014),而侵入耀岭河群的铁镁质岩墙表明新元

古代晚期构造背景主要为大陆裂谷(Zhu Xiyan et al.,2015)。因此,被动大陆边缘的沉积物不可能来自于北大巴山,根据物源方向分析,推测来自于中秦岭或北秦岭,较老沉积物经历多次搬运,沉积于北大巴山地区。

6 结论

(1)斑鸠关组主要为灰绿色细砂岩、粉砂岩和泥岩,发育粒序层理、槽模等沉积构造,沉积环境为海底扇。

(2)主量元素显示,斑鸠关组为近源堆积,主要为成熟度较低的岩屑砂屑岩。

(3)斑鸠关组物源区经历中等程度的风化作用,不具备沉积再旋回特征,物源区岩石主要为长英质火山岩。

(4)斑鸠关组砂岩地球化学综合表明,碎屑岩主要来自于北部,形成于与大陆岛弧相关的构造环境。

致谢:本文地球化学测试工作在国家地质实验测试中心完成,感谢马老师帮助! 同时,对匿名评审专家的建议表示感谢!

References

Ali S, Stattegger K, Garbe-Schöngerg D, Frank M, Kraft S, Kuhnt W. 2014. The provenance of Cretaceous to Quaternary sediments in the Tarfaya basin, SW Morocco: Evidence from trace element geochemistry and radiogenic Nd-Sr isotope. Journal of African Earth Sciences, 90: 64～76.

Armstrong-Altrin J S, Machain-Castillo M L, Rosales-Hoz L, Carranza-Edwars A, Sanchez-Cabeza J-A, Ruíz-Fernández A C. 2015. Provenance and depositional history of continental slope sediments in the Southwestern Gulf of Mexico unraveled by geochemical analysis. Continental Shelf Research, 95: 15～26.

Bhatia M R, Crook K A W. 1986. Trace element characteristics of graywackes and tectonic setting discrimination of sedimentary basins. Contributions to Mineralogy and Petrology, 92: 181～193.

Bhatia M R. 1983. Plate tectonics and geochemical composition of sandstones. The Journal of Geology, 91: 611～627.

Bhatia M R. 1985. Rare earth element geochemistry of Australian Paleozoic graywackes and mudrocks: Provenance and tectonic control. Sedimentary Geology, 45: 97～113.

Bock B, McLennan S M, Hanson G N. 1998. Geochemistry and provenance of the Middle Ordovician Austin Glen Member (Normanskill Formation) and the Taconian Orogeny in New England. Sedimentology, 45: 635～655

Chen Gaochao, Zhang Qingsheng, Kong Wennian, Ren Juangang, Peng Junying, Zhang Yuanfeng. 2011. Mineral characteristics and exploration prospect of vanadium deposit of Lower Cambrian black rock series in South Qinling East Segment. Northwestern Geology, 44(4): 50～57 (in Chinese with English abstract).

Chen Youzhang, Liu Shuwen, Li Qiugen, Dai Junzhi, Zhang Fan, Yang Pengtao, Guo Lishuang. 2010. Geology, geochemistry of Langao mafic volcanic rocks in South Qinling orogenic belt and its tectonic implications. Acta Scientiarum Naturalium Uniersitatis Pekinensis, 46 (4): 607～619 (in Chinese with English abstract).

Cox R, Lowe D R, Cullers R L. 1995. The influence of sediment recycling and basement composition on evolution of mudrock chemistry in the southwestern United States. Geochimica et Cosmochimica Acta, 59(14): 2919～2940.

Dong Yunpeng, Liu Xiaoming, Neubauer F, Zhang Guowei, Tao Ni, Zhang Yiguo, Zhang Xiaoning, Li Wei. 2013. Timing of Paleozoic amalgamation between the North China and South China Blocks: Evidence from detrital zircon U - Pb ages. Tectonophysics, 586: 173～191.

Fedo C M, Nesbitt H W, Young, G M. 1995. Unraveling the effects of potassium metasomatism in sedimentary rocks and paleosols, with implications for paleoweathering conditions and provenance. Geology, 23: 921～924.

Floyd P A, Leveridge B E. 1987. Tectonic environment of the the Devonian Gramscatho basin, south Cornwall: Framework mode and geochemical evidence from turbiditic sandstones. Journal of the Geological Society, London, 144: 531～542.

Floyd, P A, Shail R, Leveridge B E, Franke W. 1991. Geochemistry and provenance of Rhenohercynian synorogenic sandstones: Implications for tectonic environment discrimination. Geological Society of London, Special Publication, 57: 173～188.

Fu Lipu, Song Lisheng. 1986. Stratigraphy and paleontology of Silurian in Ziyang region (transitional belt). Bull. Xi'an Inst. Geol. Min. Res., Chinese Acad. Geol. Sci., (14): 1～198 (in Chinese with English abstract).

Fu Lipu, Zhang Zifu, Geng Liangyu. 2006. Silurian high resolution graptolite biostratigraphy and biotic recovery in Ziyang, China. Beijing: Geological Publishing House, 1～149 (in Chinese with English abstract).

Fu Lipu, Zhang Zifu, Xie Congrui. 2004. Cyrtograptid zones near the lower boundary of the Silurian Wenlock series in Ziyang, Shaanxi. Geological Bulletin of China, 23(8): 795～798 (in Chinese with English abstract).

Fu Lipu. 1983. Silurian stratigraphy in Bajiaokou Ziyang, Shaanxi. Bull. Xi'an Inst. Geol. Min. Res., Chinese Acad. Geol. Sci., (14): 1～198 (in Chinese with English abstract).

Gao Changlin. 1993. Study on the geochemistry of the two types of palaeo-continental margins in the middle Inner Mongolia and the east part of southern Shaanxi, China. Wuhan: China University of Geosciences Press, 45～77 (in Chinese with English abstract).

Garzanti E, Doglioni C, Vezzoli G, Andò S. 2007. Orogenic belts and orogenic sediment provenance. The Journal of Geology, 115: 315～334.

Ge Meiyu, Li Chonglou. 1984. Silurian graptolite - bearing strata in Ziyang, southern Shaanxi. Bull. Nanjing Inst. Geol. & Palaeont., Acad. Sinica, (9): 145～168 (in Chinese with English abstract).

Georgiopoulou A, Wynn R B, Masson D G, Frenz, M. 2009. Linked turbidite - debrite resulting from recent Sahara Slide headwall reactivation. Marine and Petroleum Geology, 26: 2021～2031.

Gu X X, Liu J M, Zheng J H, Tang J X, Qi L. 2002. Provenance and tectonic setting of the Proterozoic turbidites in Hunan, South China: Geochemical evidence. Journal of Sedimentary Research, 72: 393～407.

Haughton P D W, Barker S P, McCaffrey W D. 2003. 'Linked' debrites in sand-rich turbidite systems - origin and significance. Sedimentology, 50: 459～482.

Herron M M. 1988. Geochemical classification of terrigenous sands and shales from core or log data. Journal of Sedimentary Research, 58: 820～829.

Huang Yuehua, Ren Youxiang, Xia Linqi, Xia Zuchun, Zhang Cheng. 1992. Early Palaeozoic bimodal igneous suite on Northern Daba Mountains—Gaotan diabase and Haoping trachyte as examples. Acta Petrologica Sinica, 8(3): 243～256 (in Chinese with English abstract).

Johnsson M J. 1993. The system controlling the composition of clastic sediments. In Johnsson M J, Basu A (eds.) Processes controlling the composition of clastic sediments. Geological Society of America Special Publication, 284: 1～20.

Jorge R C G S, Fernandes P, Rodrigues B, Pereira Z, Oliveira J T. 2013. Geochemistry and provenance of the Carboniferous Baixo Alentejo Flysch Group, South Portuguese Zone. Sedimentary Geology, 284 - 285: 133～148.

Lei Min, Wu Cailai, Wu Xiuping, Gao Yuanhong, Wu Suoping, Chen Qilong, Qin Haipeng. 2011. Zircon SHRIMP U-Pb datings of granite and its enclave from Xinyuan pluton, Southern Qinling Mountains, and their geological significances. Geological Review, 57(6): 889～899(in Chinese with English abstract).

Lin Baoyu, Su Yangzheng, Zhu Xiufang, Rong Jiayu. 1998. Stratigraphy of China: Silurian. Beijing: Geological Publishing House, 32～33 (in Chinese without English abstract).

Lin Zhenwen, Qin Yan, Zhou Zhenju, Yue Suwei, Zeng Qingtao, Wang Lixin. 2013. Zircon U-Pb dating and geochemistry of the volcanic rocks at HuaChanggou area, Mian-Lue suture, South Qinling. Acta Petrologica Sinica, 29(1): 83～94 (in Chinese with English abstract).

Long Xiaoping. Yuan Chao, Sun Min, Xiao Wenjiao, Wang Yujing, Cai Keda, Jiang Yingde. 2012. Geochemistry and Nd isotopic composition of the Early Paleozoic flysch sequence in the Chinese Altai, Central Asia: Evidence for a northward-derived mafic source and insight into Nd model ages in accretionary orogen. Gondwana Research, 22: 554～566.

Lowe D R, Guy M, Palfrey A. 2003. Facies of slurry-flow deposits, Britannia Formation (Lower Cretaceous), North Sea: implications for flow evolution and deposit geometry. Sedimentology, 50: 45～80.

Lowe D R. 1982. Sediment gravity flows: Ⅱ. Depositional models with special references to the deposits of high-density turbidity currents. Journal of Sedimentary Petrology, 52: 279～297.

Ma Runhua, Yi Kunying, Wang Zhendong, Yao Hengxing, Shi Bingde, Yang Yingzhang, Guo Hongxiang. 1998. Lithostratigraphy of Sichuan Provinces. Wuhan: China University of Geosciences Press, 104～105 (in Chinese).

McCaffrey W, Kneller B. 2001. Process controls onthe development of stratigraphic trap potential on the margins of confined turbidite systems and aids to reservoir evaluation. AAPG Bulletin, 85: 971～988.

McLenna S M, Hemming S, McDaniel D K, Hanson G N. 1993. Geochemical approaches to sedimentation, provenance, and tectonic. GSA Special Publication, 284: 21～40.

McLennan S M, Bock B, Hemming S R, Hurowitz J A, Lev S M, McDaniel D K. 2003. The roles of provenance and sedimentary processes in the geochemistry of sedimentary rocks. In Lentz D R. (eds.) Geochemistry of sediments and sedimentary rocks: Evolutionary considerations to mineral deposit-forming environments. Geological Association of Canada, Geotext, 4: 7～38.

McLennan S M, Hemming S R, Taylor S R and Erikkson K A. 1995. Early Proterozoic crustal evolution: Geochemical and Nd-Pb isotopic evidence from metasedimentary rocks, southwestern North America. Geochimica et Cosmochimica Acta, 59: 1153～1177.

McLennan S M, Taylor S R. 1991. Sedimentary rocks and crustal evolution: Tectonic setting and secular trends. The Journal of Geology, 99: 1～21.

McLennan S M. 1989. Rare earth elements in sedimentary rocks: Influence of provenance and sedimentary processes. Reviews in Mineralogy and Geochemistry, 21: 169～200.

McLennan S M. 2001. Relationships between the trace element composition of sedimentary rocks and upper continental crust. Geochemistry Geophysics Geosystems, 2, 1021, doi: 10.1029/2000GC000109.

Nardin T R, Hein F J, Gorsline D S, Edwards B D. 1979. A review of mass-movement processes, sediment acoustic characteristics, and contrasts in slope and base of slope systems versus canyon-fan-basin floor systems. In Doyle L J, Pilkey O H. (eds.) Geology of continental slopes. SEPM special Publication, 27: 61～73.

Nesbitt H W, Young G M. 1984. Prediction of some weathering trends of plutonic and volcanic rocks based on thermodynamic and kinetic considerations. Geochimica et Cosmochimica Acta, 48: 1523～1534.

Pettijohn F J, Potter P E, Siever R. 1972. Sand and sandstones. New York: Springer-Verlag, 1-618.

Roser B P, Korsch R J. 1986. Determination of tectonic setting of sandstone-mudstone suites using SiO_2 content and K_2O/Na_2O ration. The Journal of Geology, 94: 635～650.

Roser B P, Korsch R J. 1988. Provenance signatures of sandstone-mudstone suites determined using discriminant function analysis of major-element data. Chemical Geology, 67: 119～139.

Roser B P. 2000. Whole-rock geochemical studies of clastic sedimentary suites. Memoirs of the Geological Society of Japan, 57: 73～89.

Shanmugam G. 2016. Submarine fans: A critical retrospective (1950-2015). Journal of Palaeogeography, 5: 110～184.

Sun Weidong, Li Shuguang, Chen Yadong, Li Yujing. 2003. Timing of syn-orogenic granitoids in the South Qinling, Central China: Constrains onthe evolution of the Qinling-Dabie orogenic belt. The Journal of Geology, 11: 457～468.

Talling P J, Amy L A, Wynn R B, Peakall J, Robinson M. 2004. Beds comprising debrite sandwiched within co-genetic turbidite: Origin and widespread occurrence in distal depositional environments. Sedimentology, 51: 163～194.

Talling P J, Masson D G, Sumner E J, Malgesini G. 2012. Subaqueous sediment density flows: Depositional processes and deposit types. Sedimentology, 59: 1937～2003.

Taylor S R, McLennan S M. 1985. The continenalt crust: Its composition and evolution. Blackwell Scientific Publications, Oxford

Teng Renlin, Li Yujing. 1990. Onthe lithochemical features and the diagenetic environment of the Caledonian magmatic rocks in the Northern Dabashan, Shaanxi Province. Geology of Shaanxi, 8(1): 37～52 (in Chinese with English abstract).

Wan Jun, Liu Chengxin, Yang Cheng, Liu Wanliang, Li Xiongwei, Fu Xiaojuan, Liu Hongxian. 2016. Geochemical characteristics and LA-ICP-MS zircon U-Pb age of the trachytic volcanic rocks in Zhushan area of Southern Qinling Mountains and their significance. Geological Bulletin of China, 35(7): 1134～1143 (in Chinese with English abstract).

Wang Cunzhi, Yang Kunguang, Xu Yang, Cheng Wangqiang. 2009. Geochemistry and LA-ICP-MS zircon U-Pb age of basic dike swarms in North Daba Mountains and its tectonic significance. Geological Science and Technology Information, 28(3): 19～26 (in Chinese with English abstract).

Wang Gang, Wang Zongqi, Zhang Yingli, Wang Kunming, Wu Yudong. 2017. Devonian alkaline magmatism in South Qinling, China: Evidence from the Taohekou Formation, Northern Daba Mountain. International Geology Review, 59: 1737～1763.

Wang Gang. 2014. Metallogeny of the Mesozoic and Paleozoic volcanic igneous event in Ziyang-Langao areas, North Daba Mountain. Doctor thesis: China University of Geosciences (in Chinese with English abstract).

Wang Kunming, Wang Zongqi, Zhang Yingli, Wang Gang. 2015. Geochronology and geochemistry of mafic rocks in the Xuhe, Shaanxi, China: Implications for petrogenesis and mntle dynamics. Acta Geologica Sinica (English Edition), 89: 187～202.

Wang Kunming, Wang Zongqi, Zhang Yingli, Wang Gang. 2016. Determination of kaersutite and its implication for mafic rock in Taohe area, North Daba Mountain. Acta Petrologica et Mineralogica, 35(3): 506～516 (in Chinese with English abstract).

Wang Wei, Zhou Meifu. 2013. Petrological and geochemical constraints on provenance, paleoweathering, and tectonic setting of the Neoproterozoic sedimentary basin in the eastern Jiangnan

Orogen, South China. Journal of Sedimentary Research, 83: 975～994.

Wang Zongqi, Yan Quanren, Yan Zhen, Wang Tao, Jiang Chunfa, Gao Lianda, Li Qiugen, Chen Junlu, Zhang Yingli, Liu Ping, Xie Chunlin, Xiang Zhongjin. 2009. New division of the main tectonic units of the Qinling orogenic belt, Central China. Acta Geologica Sinica, 83(11): 1527～1546 (in Chinese with English abstract).

Winchester J A, Floyd P A. 1977. Geochemical discrimination of different magma series and their differentiation products using immobile elements. Chemical Geology, 20: 325～343.

Xia Zuchun, Xia Linqi, Zhang Cheng. 1992. The study of pyroxene minerals of alkali-basic-ultrabasic subvolcanic complex from North Daba Mountain. Northwest Geoscience, 13(2): 23～30 (in Chinese with English abstract).

Xiang Zhongjin, Yan Quanren, Song Bo, Wang Zongqi. 2016. New evidence for the ages of ultramafic to mafic dikes and alkaline volcanic complexes in the North Daba Mountains and its geological implication. Acta Geologica Sinica, 90(5): 896～916 (in Chinese with English abstract).

Xiang Zhongjin, Yan Quanren, Yan Zhen, Wang Zongqi, Wang Tao, Zhang Yingli, Qin Xiaofeng. 2010. Facies succsssion and architecture of volcaniclastic rocks of the Taohekou Formation: Implication for Early Silurian volcanism in the North Dabashan area, China. Acta Geologica Sinica, 84(3): 311～328 (in Chinese with English abstract).

Xiong Guoqing, Wang Jian, Li Yuanyuan, Yu Qian, Men Yupeng, Zhou Xiaolin, Xiong Xiaohui, Zhou Yexin, Yang Xiao. 2017. Lithofacies palaeogeography of the Early Paleozoic black rock series in Dabashan region and their shale-gas geological significance. Journal of Palaeogeography, 19(6): 965～986(in Chinese with English abstract).

Xu Guang, Wang Kunming, Wang Zongqi, Zhang Yingli, Wang Gang, Wu Yudong. 2018. Geochemistry and geochronology of Hualicun mafic rocks in North Daba Mountain and tectonic control. Geological Bulletin of China, 37(7): 1279～1290 (in Chinese with English abastract).

Yan Zhen, Wang Zongqi, Chen Junlu, Yan Quanren, Wang Tao. 2010. Detrital record of Neoproterozoic arc-magmatism along the NW margin ofthe Yangtze Block, China: U-Pb geochronology and petrography of sandstones. Journal of Asian Earth Sciences, 37: 322～334.

Yan Zhen, Wang Zongqi, Yan Quanren, Wang Tao, Guo Xianqing. 2012. Geochemical constraints onthe provenance and depositional setting of the Devonian Liuling Group, East Qinling Mountains, Central China: Implications for the tectonic evolution of the Qinling orogenic belt. Journal of Sedimentary Research, 82: 9～20.

Yan Zhen, Wang Zongqi, Yan Quanren, Wang Tao, Xiao Wenjiao, Li Jiliang, Han Fanglin, Chen Junlu, Yang Yongcheng. 2006. Devonian sedimentary environments and procenances of the Qinling orogen: Constraints on Late Paleozoic southward accretion of the North China craton. International Geology Review, 48: 585～618.

Yan Zhen, Wang Zongqi, Zhang Yingli, Xiang Zhongjin, Yan Quanren, Wang Tao. 2011. Sedimentary features and tectonic environments of Silurian volcanic-related carbonates inthe North Daba Mountains. Acta Sedimentologica Sinica, 29(1): 31～40 (in Chinese with English abstract).

Yang Cheng, Liu Chengxin, Liu Wanliang, Wan Jun, Duan Xianfeng, Zhang Zhong. 2017. Geochemical characteristics of trachyte and Nb mineralization process in Tianbao township, Zhuxi County, Southern Qinling. Acta Petrologica et Mineralogica, 36(5): 605～618 (in Chinese with English abstract).

Zhang Cengli, Gao Shan, Zhang Guowei, Liu Xiaoming, Yu Zaiping. 2003. Geochemistry of early Paleozoic alkali dyke swarms in south Qinling and its geological significance. Science in China (Series D), 46(12): 1292～1306.

Zhang Chengli, Gao Shan, Yuan Honglin, Zhang Guowei, Yan Yunxiang, Luo Jinglan, Luo Jinhai. 2007. Sr-Nd-Pb isotopes of the Early Paleozoic maficultrama-fic dykes and basalts from South Qinling belt and their implications for mantle composition. Science China Earth Sciences, 50(9): 1293～1301.

Zhang Chengli, Wang Tao, Wang Xiaoxia. 2008. Origin and tectonic setting of the Early Mesozoic granitoids in Qinling orogenic belt. Geological Journal of China Universities, 14(3): 304～316 (in Chinese with English abstract).

Zhang Guishan, Liu Shuwen, Han Wenhua, Zheng Houyi. 2017. Baddeleyite U - Pb age and geochemical data of the mafic dykes from South Qinling: Constraints on the lithospheric extension. Geological Journal, 52(S1): 272～285.

Zhang Yingli, Wang Zongqi, Wang Gang, Wang Kunming. 2016. Detrital zircon geochronology of the Late Paleozoic Taohekou Formation and its constraints on the Paleozoic magmatic events in North Daba Mountains. Acta Geologica Sinica, 90(4): 728～738 (in Chinese with English abstract).

Zhu Xiyan, Chen Fukun, Liu Bingxiang, Zhang He, Zhai Minguo. 2015. Geochemistry and zircon ages of mafic dikes in the South Qinling, central China: Evidence for late Neoproterozoic continental rifting in the northern Yangtze block. International Journal of Earth Science, 104: 27～44.

Zhu Xiyan, Chen Fukun, Nie Hu, Siebel W, Yang Yizeng, Xue Yingyu, Zhai Mingguo. 2014. Neoproterozoic tectonic evolution of South Qinling, China: Evidence from zircon ages and geochemistry ofthe Yaolinghe volcanic rocks. Precambrian Research, 245: 115～130.

Zou Xianwu, Duan Qifa, Tang Chaoyang, Cao Liang, Cui Sen, Zhao Wuqiang, Xia Jie, Wang Lei. 2011. SHRIMP zircon U-Pb dating and lithogeochemical characteristics of diabase from Zhenping area in North Daba Mountain. Geology in China, 38(2): 282～291 (in Chinese with English abstract).

参 考 文 献

陈高潮,张清盛,孔文年,任娟岗,彭俊英,张元丰. 2011. 南秦岭东段下寒武统黑色岩系钒矿成矿地质背景浅析. 西北地质,44(4):50～57.

陈友章,刘树文,李秋根,代军治,张帆,杨朋涛,郭丽爽. 2010. 南秦岭岚皋基性火山岩的地质学、地球化学及其构造意义. 北京大学学报(自然科学版),46(4):607～619.

傅力浦,宋礼生. 1986. 陕西紫阳地区(过渡带)志留纪地层及古生物. 中国地质科学院西安地质矿产研究所所刊,(14):1～198.

傅力浦,张子福,耿良玉. 2006. 中国紫阳志留系高分辨率笔石生物地层与生物复苏. 北京:地质出版社,1～149.

傅力浦,张子福,谢从瑞. 2004. 陕西紫阳志留系文洛克统底界附近弓笔石带的划分. 地质通报,23(8):795～798.

傅力浦. 1983. 陕西紫阳芭蕉口志留纪地层. 中国地质科学院西安地质矿产研究所所刊,(6):1～18.

高长林. 1993. 中国内蒙古中部和陕南东部两类古大陆边缘的地球化学研究. 武汉:中国地质大学出版社,45～77.

葛梅钰,李崇楼. 1984. 陕西紫阳瓦房店志留纪地层. 中国科学院南京地质古生物研究所丛刊,(9):145～168.

黄月华,任有祥,夏林圻,夏祖春,张诚. 1992. 北大巴山早古生代双模式火成岩套:以高滩辉绿岩和蒿坪粗面岩为例. 岩石学报,8(3):243～256.

雷敏,吴才来,武秀萍,郜源红,吴锁平,陈其龙,秦海鹏. 2011. 南秦岭新院岩体及其包体的锆石 SHRIMP U-Pb 定年和意义. 地质论评,57(6):889～899.

林宝玉,苏养正,朱秀芳,戎嘉余. 1998. 中国地层典·志留系. 北京:地质出版社,32～33.

林振文,秦艳,周振菊,岳素伟,曾庆涛,王立新. 2013. 南秦岭勉略带铧厂沟火山岩锆石 U-Pb 年代学及地球化学研究. 岩石学报,29(1):83～94.

马润华,伊鹍英,王振东,姚恒兴,史秉德,杨应章,郭洪祥. 1998. 陕西省岩石地层. 武汉:中国地质大学出版社,104～105.

滕人林,李育敬. 1990. 陕西北大巴山加里东期岩浆岩的岩石化学特征及其生成环境的探讨. 陕西地质,8(1):37～52.

万俊,刘成新,杨成,刘万亮,李雄伟,付晓娟,刘虹显. 2016. 南秦岭竹山地区粗面质火山岩地球化学特征、LA-ICP-MS 锆石 U-Pb 年龄及其大地构造意义. 地质通报,35(7):1134～1143.

王存智,杨坤光,徐扬,程万强. 2009. 北大巴基性岩墙群地球化学特征、LA-ICP-MS 锆石 U-Pb 定年及其大地构造意义. 地质科技情报,28(3):19～26.

王刚. 2014. 北大巴山紫阳—岚皋地区古生代火山岩浆事件与中生代成矿作用. 中国地质大学(北京)博士论文.

王坤明,王宗起,张英利,王刚. 2016. 北大巴山滔河镁铁质岩中钛闪石的厘定及指示意义. 岩石矿物学杂志,35(3):506～516.

王宗起,闫全人,闫臻,王涛,姜春发,高联达,李秋根,陈隽璐,张英利,刘平,谢春林,向忠金. 2009. 秦岭造山带主要大地构造单元的新划分. 地质学报,83(11):1527～1546.

夏祖春,夏林圻,张诚. 1992. 北大巴山碱质基性—超基性潜火山杂岩的辉石矿物研究. 西北地质科学,13(2):23～30.

向忠金,闫全人,宋博,王宗起. 2016. 北大巴山超基性、基性岩墙和碱质火山杂岩形成时代的新证据及其地质意义. 地质学报,90(5):896～916.

向忠金,闫全人,闫臻,王宗起,王涛,张英利,覃小锋. 2010. 北大巴山志留系滔河口组火山碎屑岩相序、组构特征及古火山作用环境分析. 地质学报,84(3):311～328.

熊国庆,王剑,李园园,余谦,门玉澎,周小琳,熊小辉,周业鑫,杨萧. 2017. 大巴山地区早古生代黑色岩系岩相古地理及页岩气地质意义. 古地理学报,19(6):965～986.

许光,王坤明,王宗起,张英利,王刚,武昱东. 2018. 北大巴山花栎村镁铁质岩地球化学、年代学及其构造环境制约. 地质通报,37(7):1279～1290.

闫臻,王宗起,张英利,向忠金,闫全人,王涛. 2011. 北大巴山与志留纪火山作用相关的碳酸盐岩沉积学特征及形成环境. 沉积学报,29(1):31～40.

杨成,刘成新,刘万亮,万俊,段先锋,张众. 2017. 南秦岭竹溪县天宝乡粗面岩地球化学特征与铌成矿. 岩石矿物学杂志,36(5):605～618.

张成立,王涛,王晓霞. 2008. 秦岭造山带早中生代花岗岩成因及其构造环境. 高校地质学报,14(3):304～316.

张英利,王宗起,王刚,王坤明. 2016. 北大巴山地区晚古生代滔河口组碎屑锆石年代学研究及对古生代岩浆事件的限定. 地质学报,90(4):728～738.

邹先武,段其发,汤朝阳,曹亮,崔森,赵武强,夏杰,王磊. 2011. 北大巴山镇坪地区辉绿岩锆石 SHRIMPU-Pb 定年和岩石地球化学特征. 中国地质,38(2):282～291.

Sandstone geochemical constraints on the provenance and tectonic setting of the Banjiuguan Formation in the North Daba Mountain

ZHANG Yingli*, WANG Zongqi, WANG Kunming, WANG Gang, WU Yudong

MNR Key Laboratory of Metallogeny and Mineral Assessment, Institute of Mineral Resources, CAGS, Beijing, 100037

* *Corresponding author: yinglizh@126.com*

Abstract

The North Dabashan Mountain, an important part of the South Qinling orogenic belt, holds well preserved sedimentary records. For a long time, the Banjiuguan Formation was considered to have formed in a relatively stable tectonic setting. In this paper, sedimentary successions and geochemical analyses are used to determine its provenance and tectonic setting. The Banjiuguan Formation consists of fine-grained sandstones, siltstones and mudstones deposited in deep waters. Facies assemblages indicate that they were deposited in a submarine fan environment. Paleocurrent data preserved in cross bedding indicates that sediments were proximally derived from north. Chemical classification of the Banjiuguan sandstones shows that the analyzed sediments are mostly litharenite. The REE patterns are characterized by LREE enrichment, flat HREE, and negative Eu anomalies. Chemical Index of Alteration range from 51 to 67, and Th/U ratio is 3.36 to 7.02, both of which suggest weak weathering. The rations of Zr/Sc and Th/Sc further show that the sandstone experienced no reworking. Various plots and parameters for sedimentary provenance show that the sediments were sourced predominantly from felsic rocks. Geochemical data suggest that they were deposited in an environment related to continental island arc setting and passive continental margin.

Key words: North Daba Mountain; Banjiuguan Formation; geochemistry; Provenance analysis; Tectonic setting